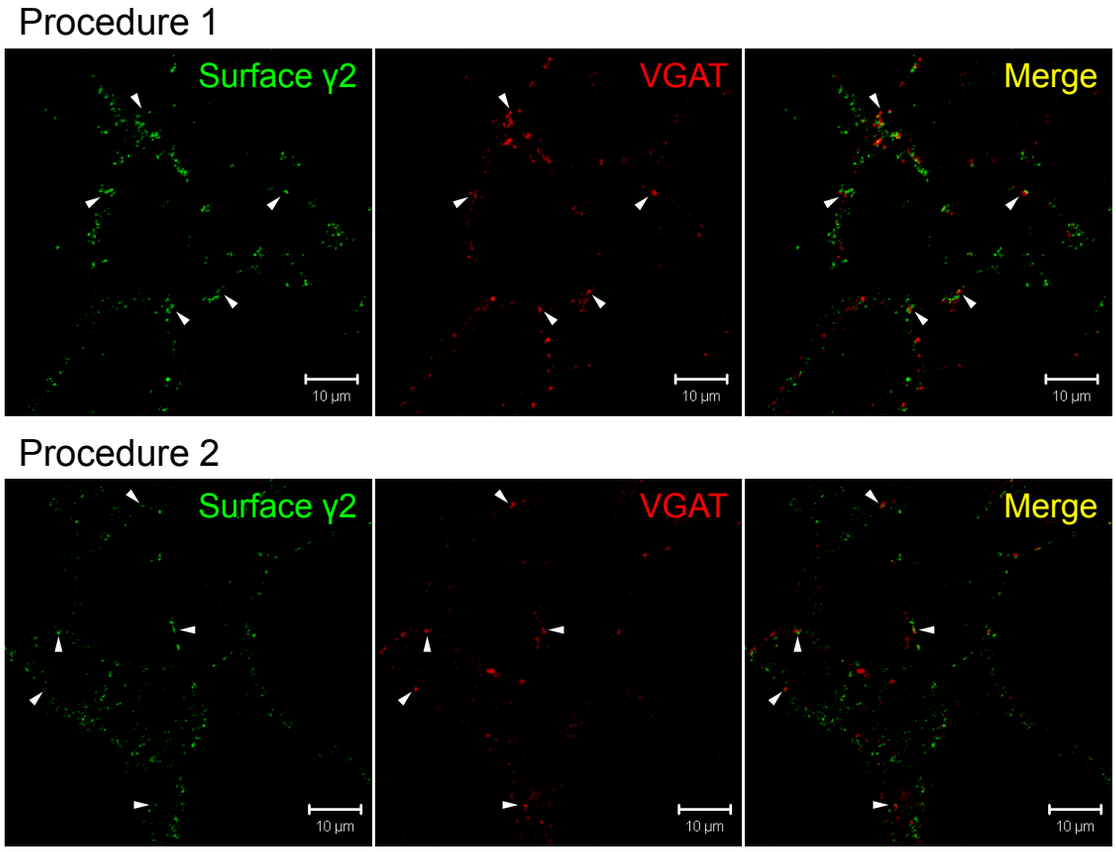
Procedure 1
Surface γ2
VGAT
Merge
10 μm
Procedure 2
Surface γ2
VGAT
Merge
10 μm

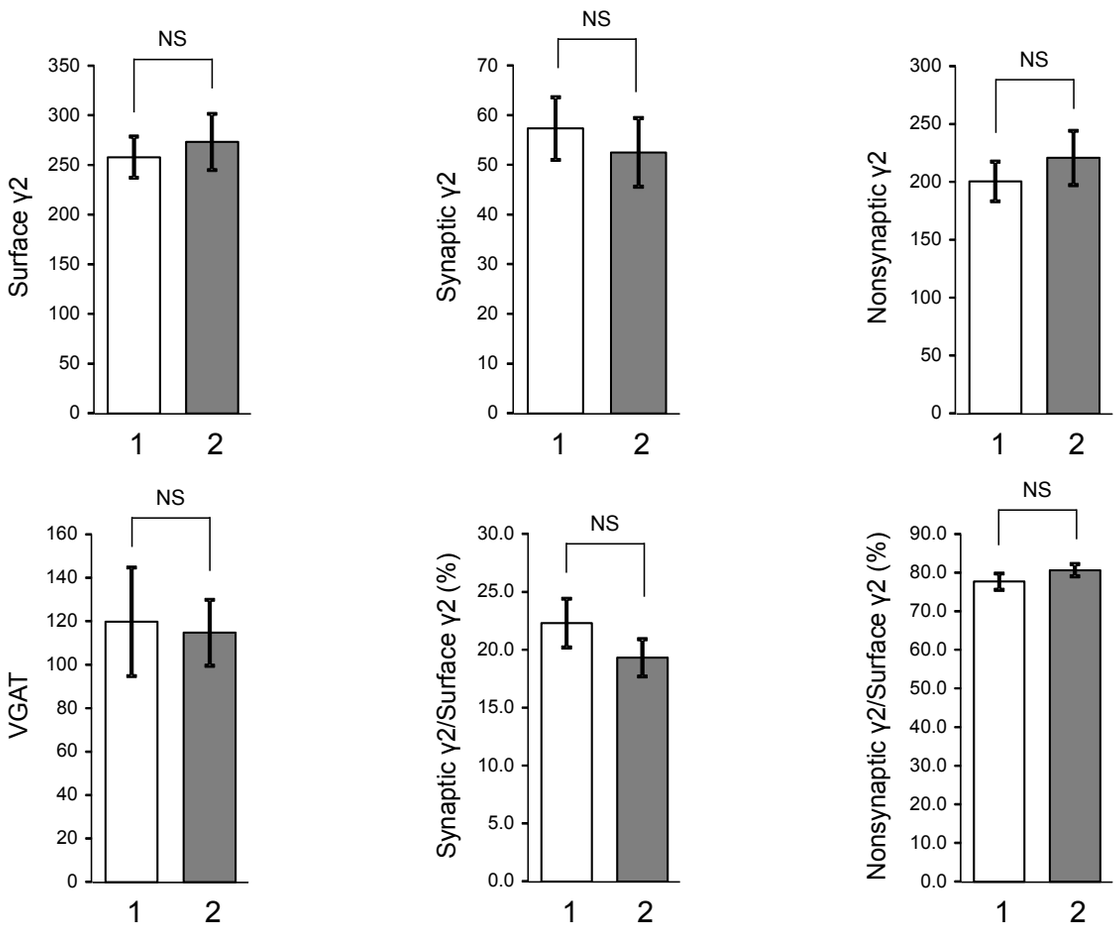
NS
Surface γ2
Synaptic γ2
Nonsynaptic γ2
VGAT
Synaptic γ2/Surface γ2 (%)
Nonsynaptic γ2/Surface γ2 (%)
1
2

Supplementary Fig. 1. Quantitative comparison of surface $GABA_AR$ localization detected with two distinct labeling procedures

Procedure 1: WT mouse hippocampal neurons (14 DIV) were labeled with a rabbit anti-γ2 antibody and then with an Alexa Fluor 488-conjugated anti-rabbit IgG antibody. After fixation and permeabilization, the neurons were stained with a mouse anti-VGAT antibody, followed by with an Alexa Fluor 594-conjugated anti-mouse IgG antibody. Procedure 2 (a control procedure): WT mouse hippocampal neurons (14 DIV) were labeled with a rabbit anti-γ2 antibody and then fixed. After labeling with an Alexa Fluor 488-conjugated anti-rabbit IgG antibody and permeabilization, the neurons were stained with a mouse anti-VGAT antibody, followed by with an Alexa Fluor 594-conjugated anti-mouse IgG antibody. Puncta of surface $GABA_ARs$ (green) that overlap with those of the presynaptic marker VGAT (red) were regarded as synaptically localized $GABA_ARs$ (arrowheads). The number of puncta was quantified using ImageJ. Data are shown as the mean ± SEM. NS, not significant (Student's *t*-test). $n = 5$ (procedure 1) and 5 (procedure 2) across two independent experiments. There was no significant difference in the number of synaptic $GABA_ARs$ and the ratio of synaptic to surface $GABA_ARs$ between the procedures. We reasoned that artificial aggregation of surface $GABA_ARs$ was kept to the minimum in our surface labeling procedure.

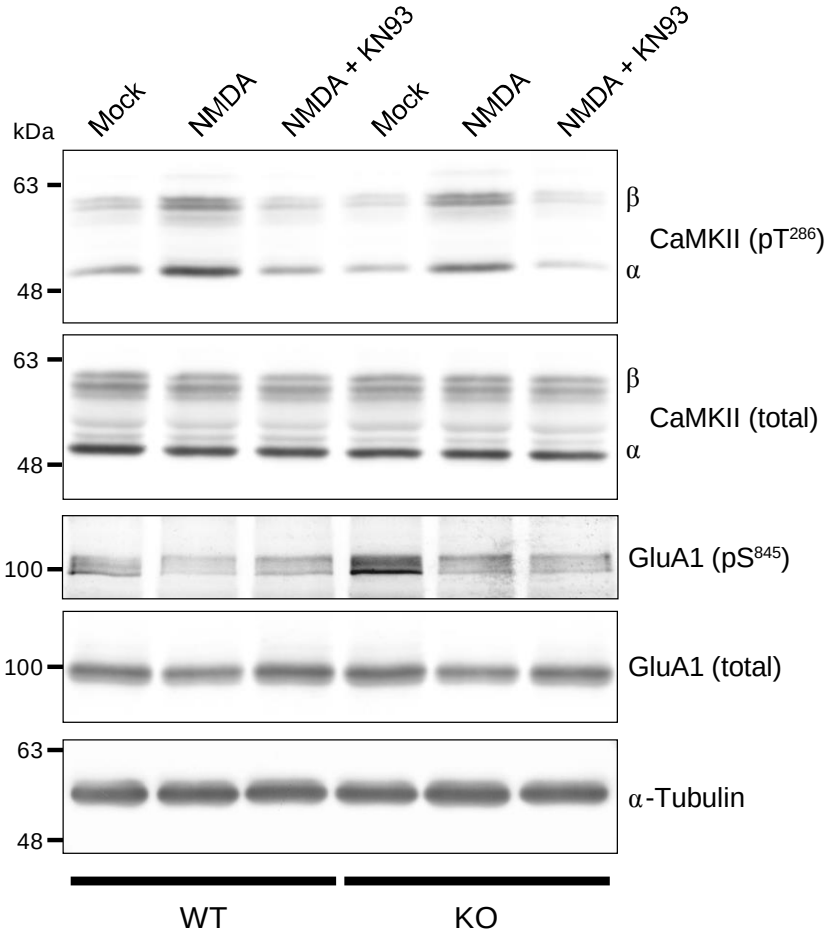

Supplementary Fig. 2. The stimulation conditions for chem-iLTP induction represent a valid experimental model

WT and KO hippocampal neurons (14 DIV) were briefly stimulated with 20 μM NMDA (plus 10 μM CNQX) for 3 min in the presence or absence of the cell-permeable CaMKII inhibitor KN93, and the cell lysates were analyzed by immunoblotting with the indicated antibodies. α-tubulin was used as a loading control. We observed two major hallmarks of chem-iLTP[27,46]: an increase in CaMKII autophosphorylated at Thr[286] and a decrease in the GluA1 subunit of α-amino-3-hydroxy-5-methyl-4-isoxazolepropionic acid receptors (AMPARs) phosphorylated at Ser[845]. Pretreatment of neurons with KN93 blocked Thr[286] phosphorylation of CaMKII, but not Ser[845] dephosphorylation of GluA1. These results validated our protocol for chem-iLTP, and we used identical conditions for the subsequent experiments.

Fig. S3

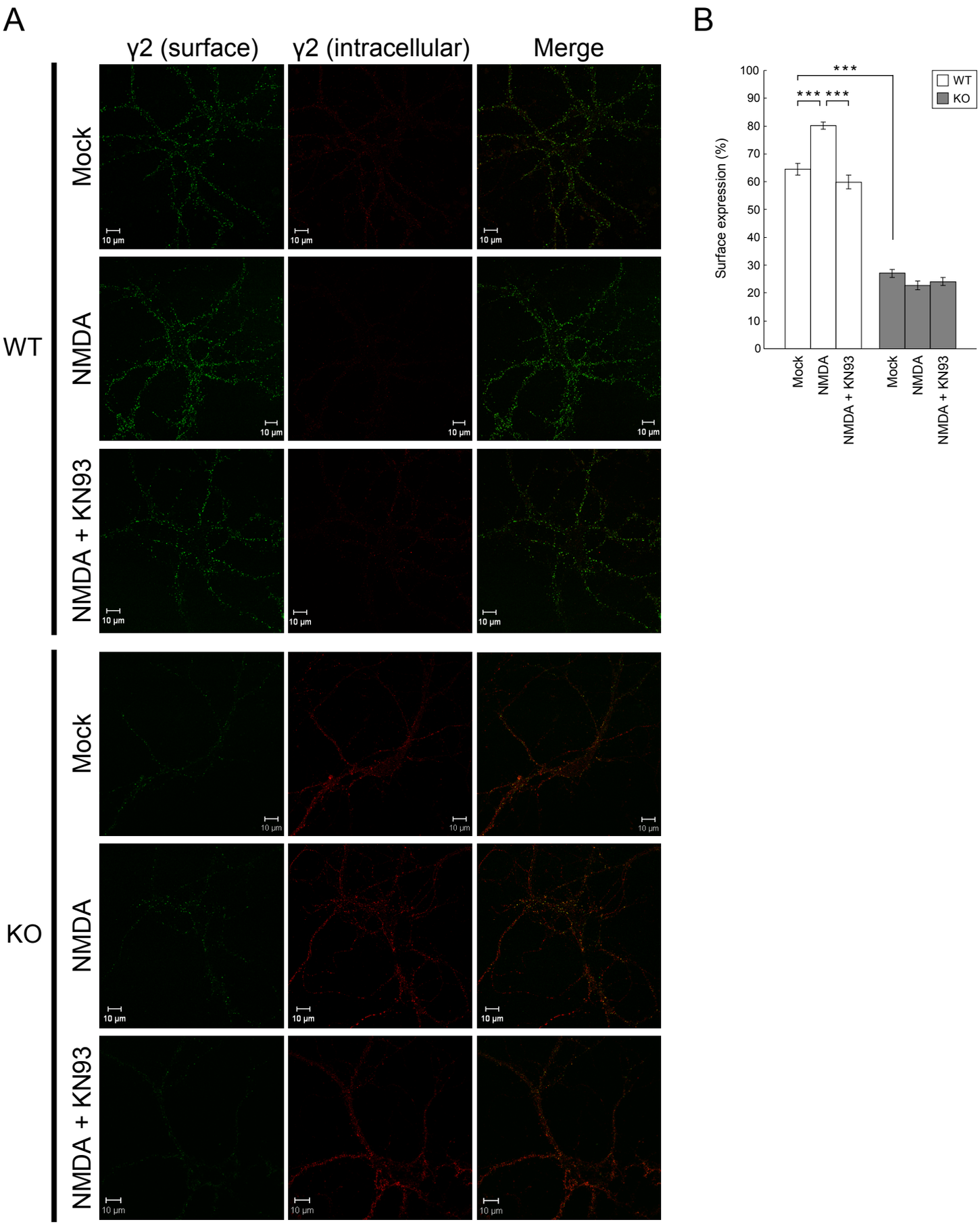
A
γ2 (surface)
γ2 (intracellular)
Merge
WT
KO
Mock
NMDA
NMDA + KN93
10 μm
B
Surface expression (%)
100
90
80
70
60
50
40
30
20
10
0
***
***
***
WT
KO
Mock
NMDA
NMDA + KN93
Mock
NMDA
NMDA + KN93

Supplementary Fig. 3. PX-RICS is required for $GABA_AR$ transport during chem-iLTP (A) WT and KO hippocampal neurons were treated with vehicle (mock) or moderately stimulated with NMDA in the presence or absence of KN93 as indicated, and surface (green) and intracellular (red) γ2 subunits were separately visualized. Scale bars, 10 μm. (B) Quantitative analyses of the γ2 fluorescent signals in the perisomatic regions. Data are shown as the mean ± SEM. ***$P < 0.001$ (Student's *t*-test). $n = 10$ (WT) and 10 (KO) across two independent experiments.

Fig. S4

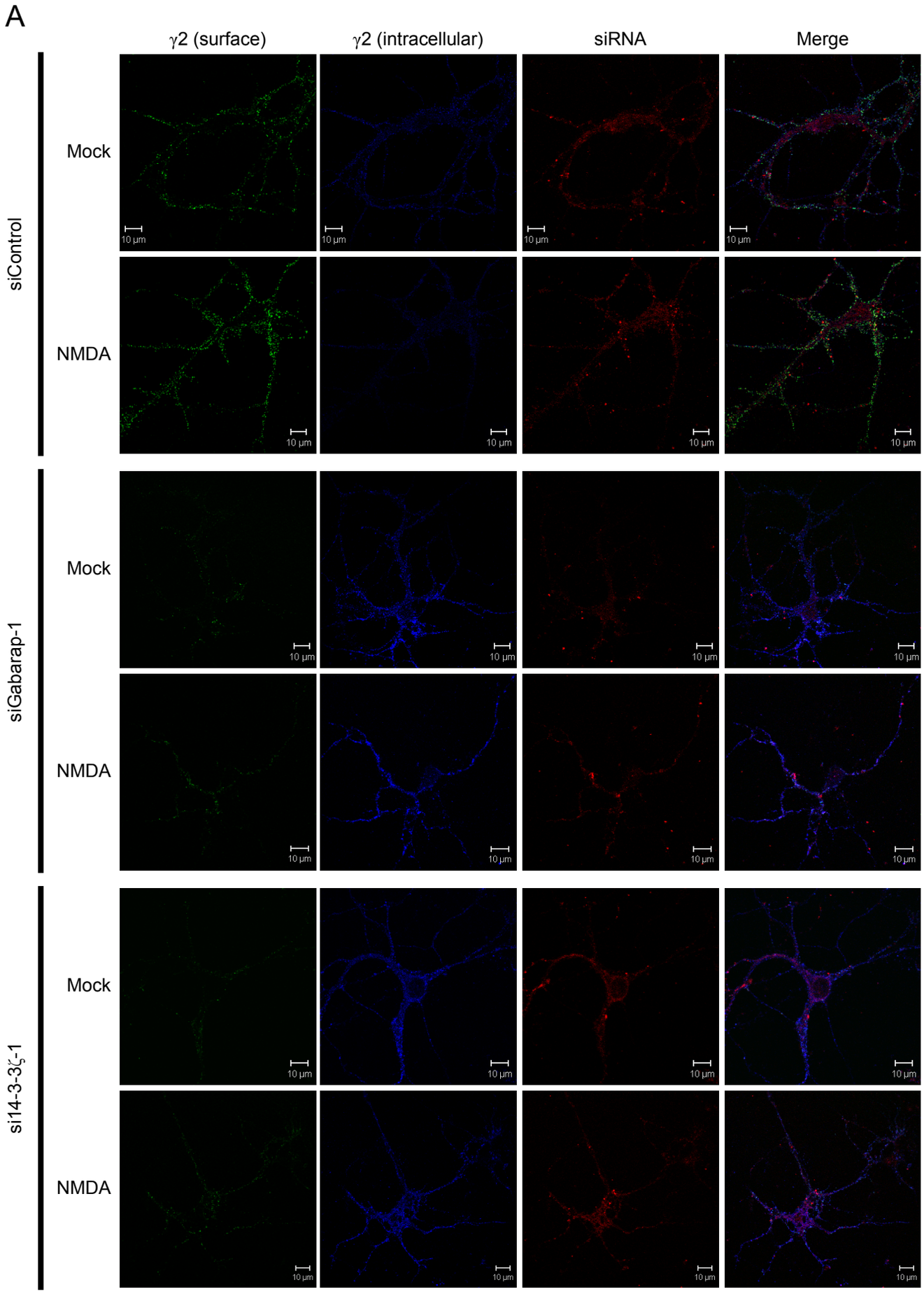
A
γ2 (surface)
γ2 (intracellular)
siRNA
Merge
siControl
siGabarap-1
si14-3-3ζ-1
Mock
NMDA
10 μm

A (continued)

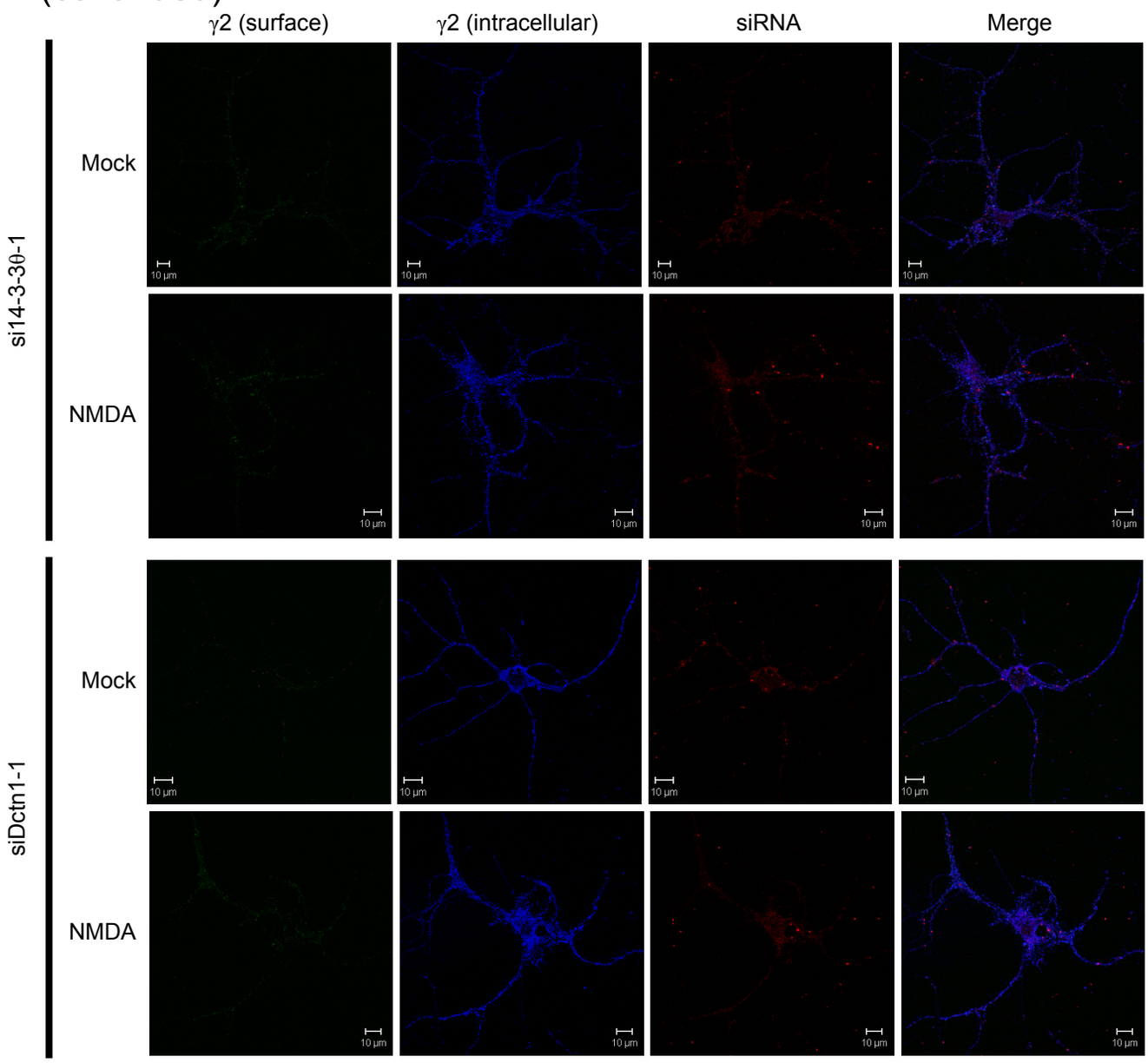

B

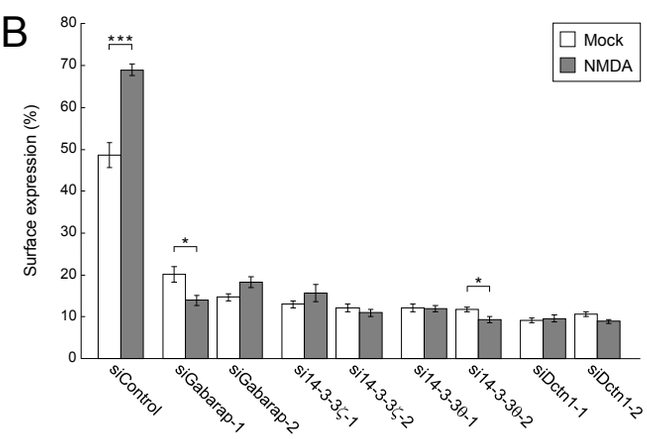

Supplementary Fig. 4. GABARAP, 14-3-3ζ/θ and dynactin1 are required for $GABA_AR$ transport during chem-iLTP

(A) WT hippocampal neurons were transfected with the indicated siRNA plus Red Fluorescent Oligo. After treatment with vehicle (mock) or low-dose NMDA, surface (green) and intracellular (blue) levels of the γ2 subunit in the perisomatic regions of siRNA-transfected neurons (red) were analyzed. Scale bars, 10 μm.

(B) Quantitative analyses of γ2 fluorescent signals in the perisomatic regions.

Data are shown as the mean ± SEM. **P* < 0.05; ****P* < 0.001 (Student's *t*-test). *n* = 10 (for each siRNA) across two independent experiments.

Fig. S5

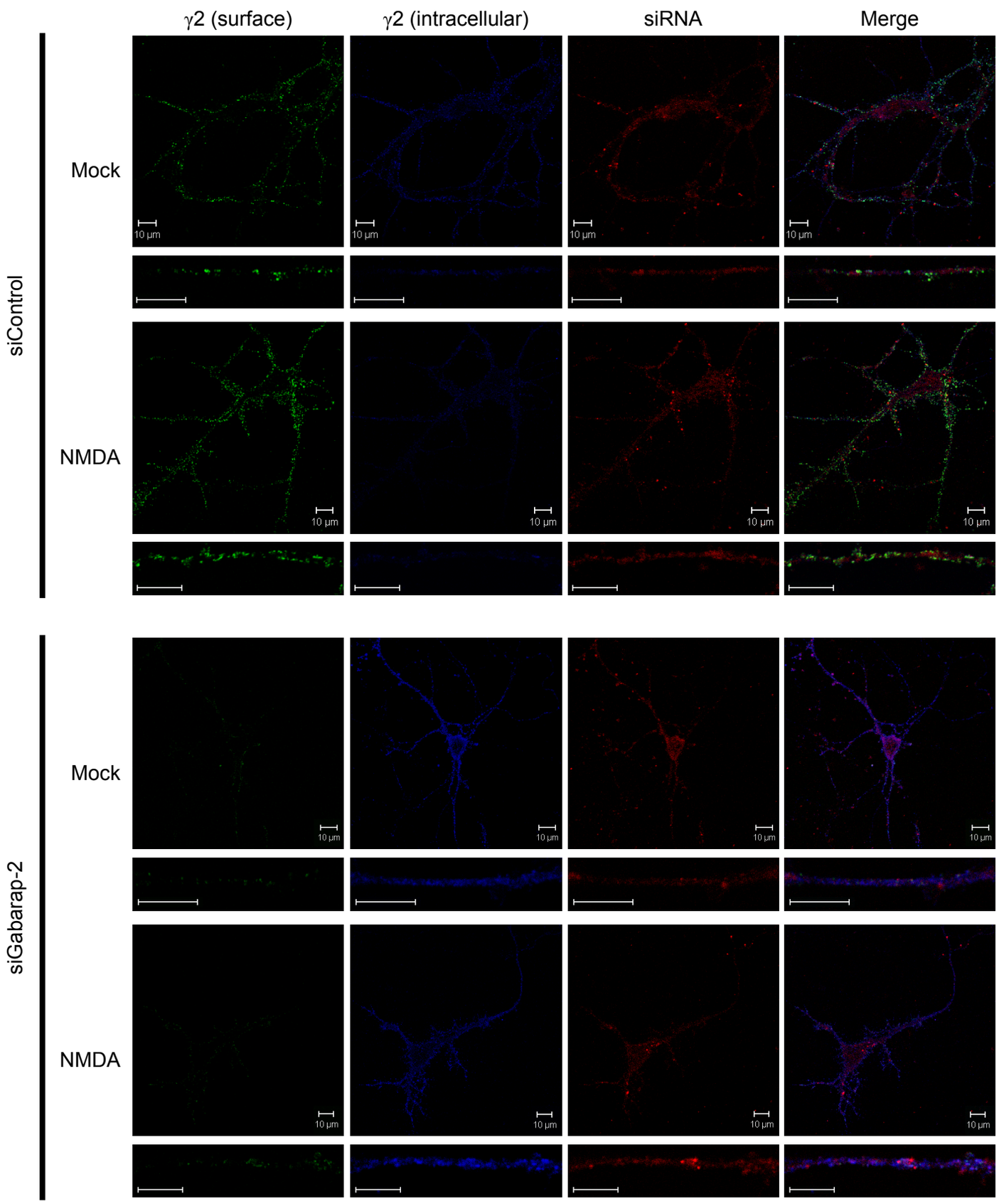
γ2 (surface)
γ2 (intracellular)
siRNA
Merge
siControl
Mock
NMDA
siGabarap-2
Mock
NMDA
10 μm

Fig. S5 (continued)

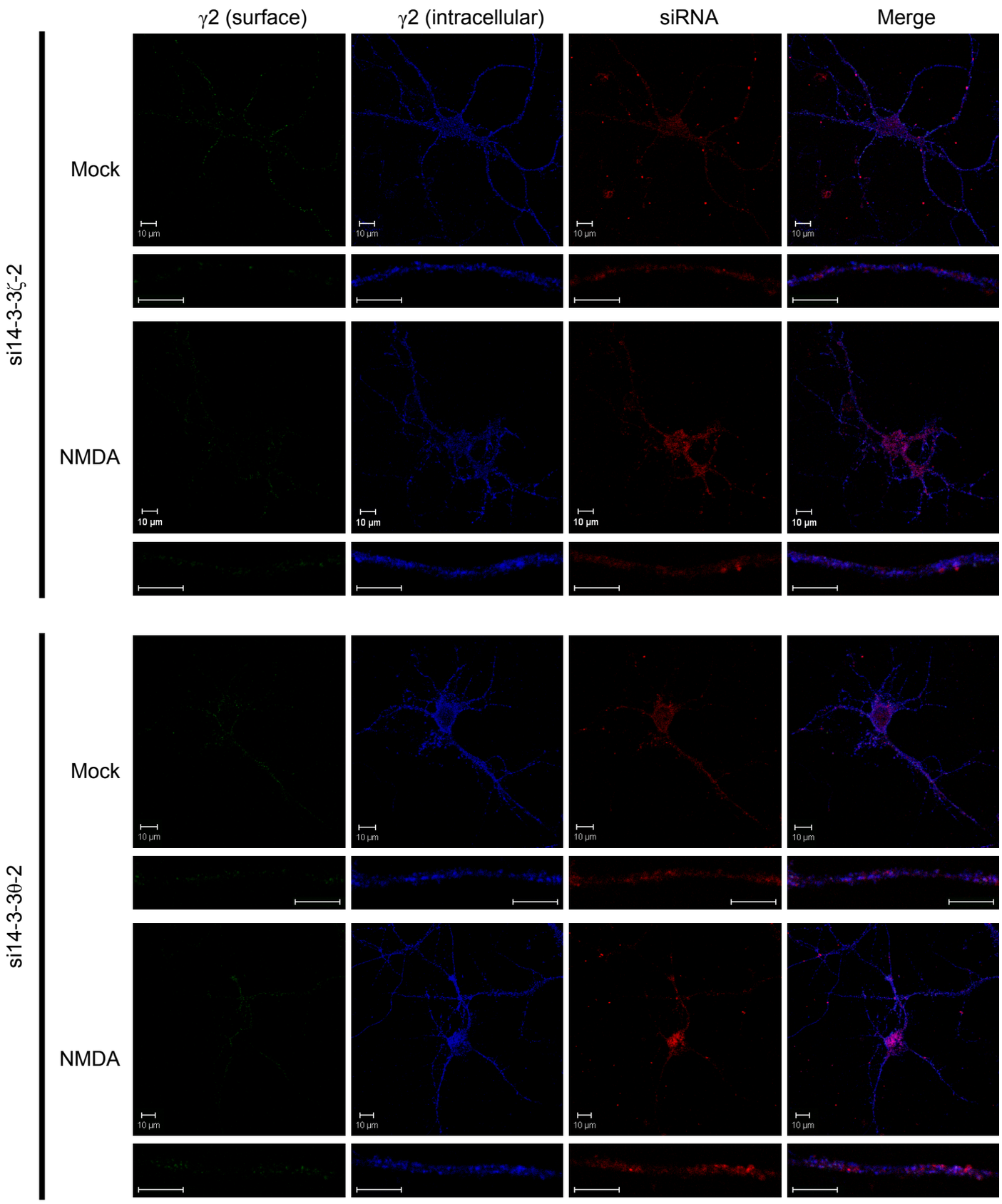

Fig. S5 (continued)

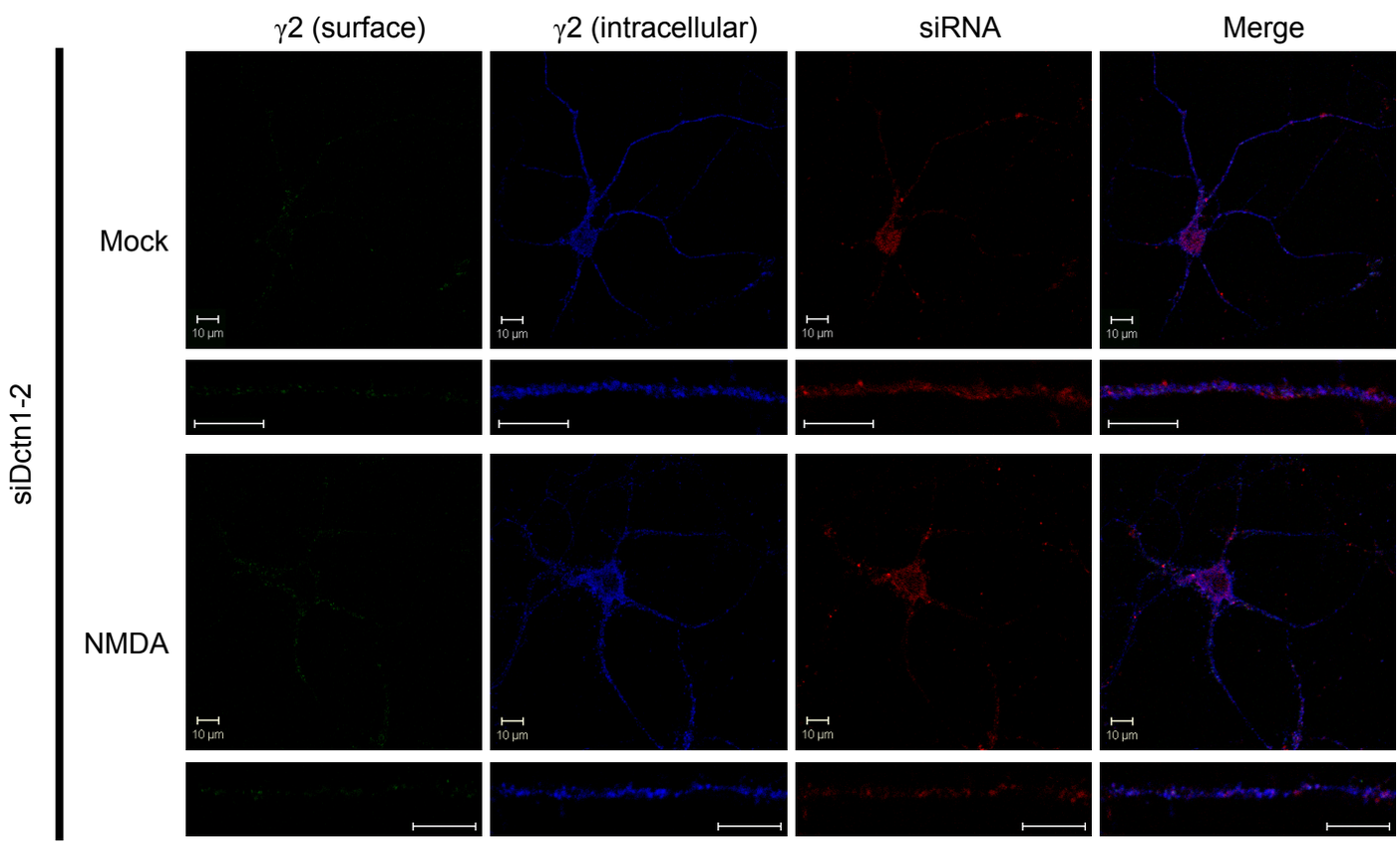

Supplementary Fig. 5. GABARAP, 14-3-3ζ/θ and dynactin1 are required for $GABA_AR$ transport during chem-iLTP

WT hippocampal neurons (10 DIV) were transfected with the indicated siRNAs, the nucleotide sequences of which are different from those used in Figure 2 although they target the same mRNAs. Red Fluorescent Oligo was co-transfected to identify siRNA-transfected neurons. After treatment with vehicle (mock) or low-dose NMDA, surface (green) and intracellular (blue) levels of the γ2 subunit in the perisomatic regions and in the distal dendrites of siRNA-transfected neurons (red) were analyzed. The quantitative data were integrated into Fig. 2B–D (the distal dendrites) and Supplementary Fig. 4B (the perisomatic regions). Scale bars, 10 μm.

Fig. S6

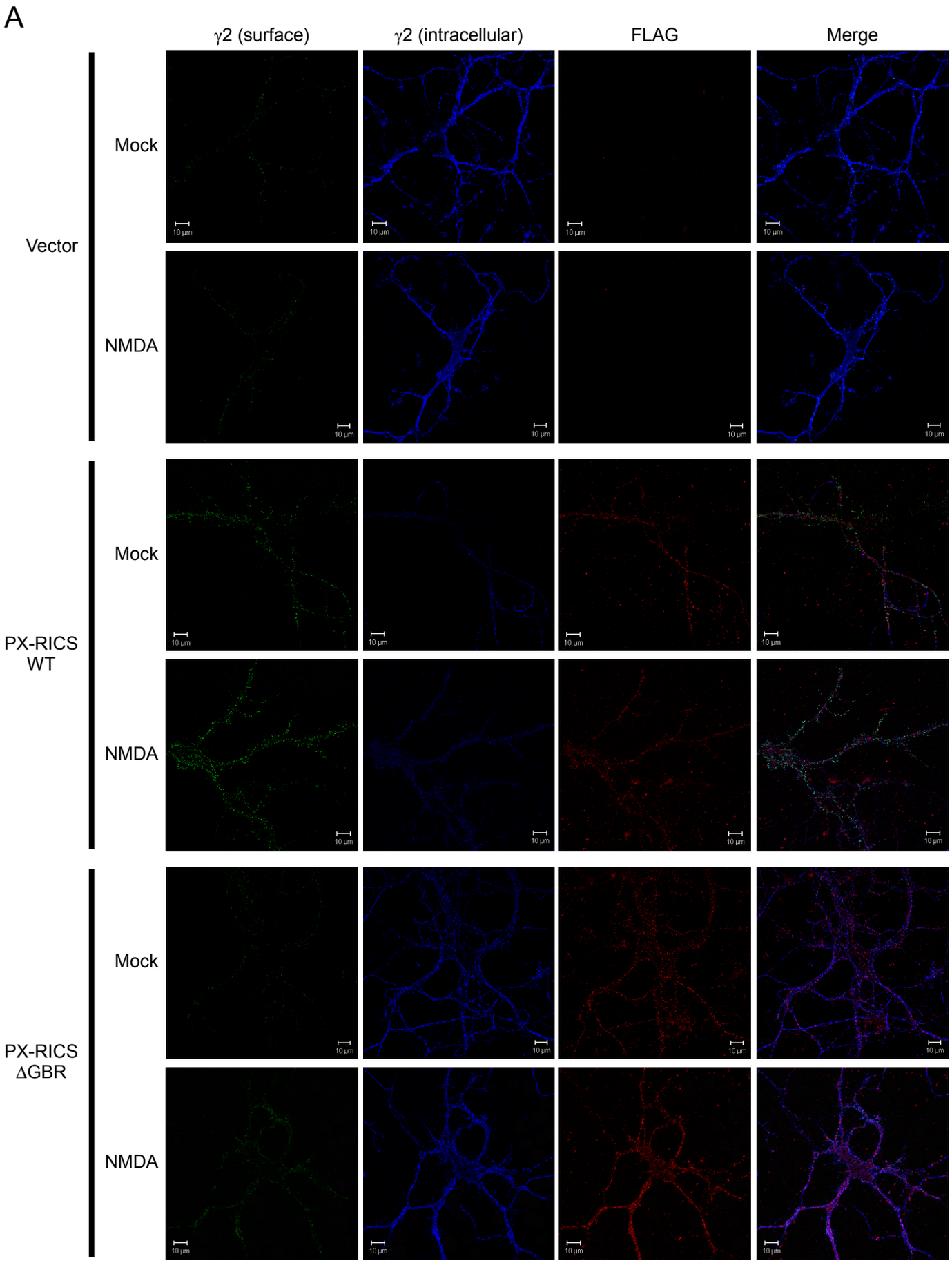
A
γ2 (surface)
γ2 (intracellular)
FLAG
Merge
Vector
Mock
NMDA
PX-RICS WT
Mock
NMDA
PX-RICS ΔGBR
Mock
NMDA
10 μm

A (continued)

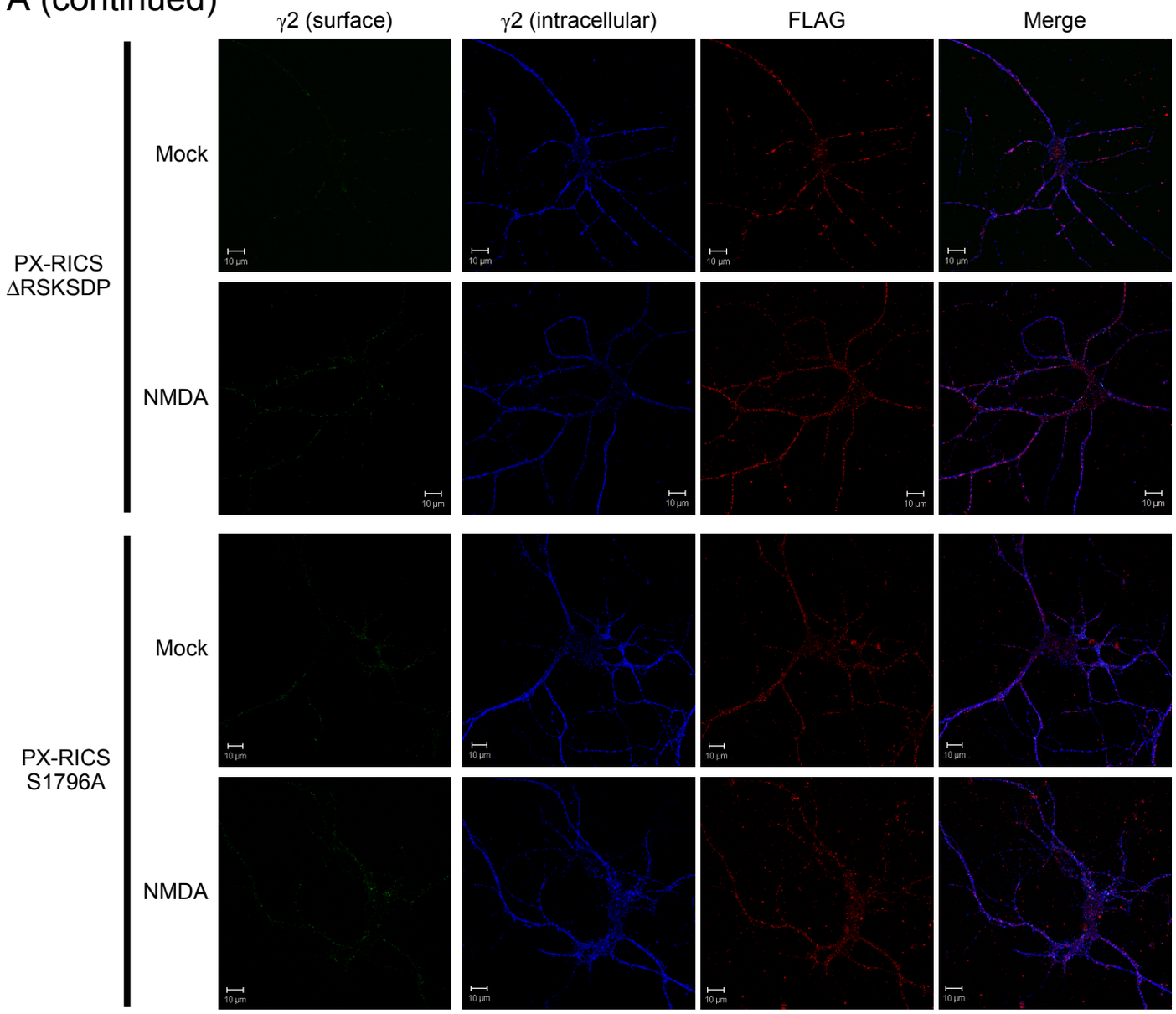

B

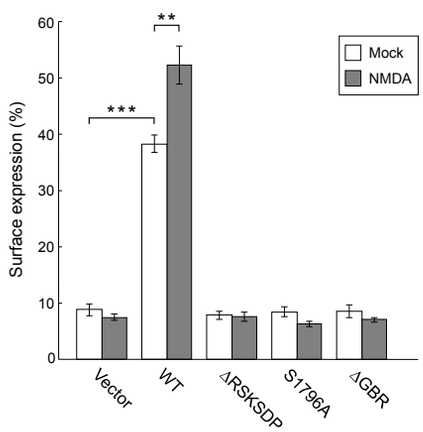

Supplementary Fig. 6. $GABA_AR$ transport during chem-iLTP requires complex formation of PX-RICS with GABARAP and 14-3-3ζ/θ

(A) KO hippocampal neurons were transfected with plasmids expressing FLAG-tagged wild-type or mutant PX-RICS as indicated. After mock or moderate NMDA stimulation, surface-expressed (green) and intracellular (blue) levels of the γ2 subunit in the perisomatic regions of transfected neurons (red) were analyzed. Scale bars, 10 μm.

(B) Quantitative analyses of γ2 fluorescent signals in the perisomatic regions.

Data are shown as the mean ± SEM. $^{**}P < 0.01$; $^{***}P < 0.001$ (Student's *t*-test). $n = 10$ (for each construct) across two independent experiments.

Fig. S7

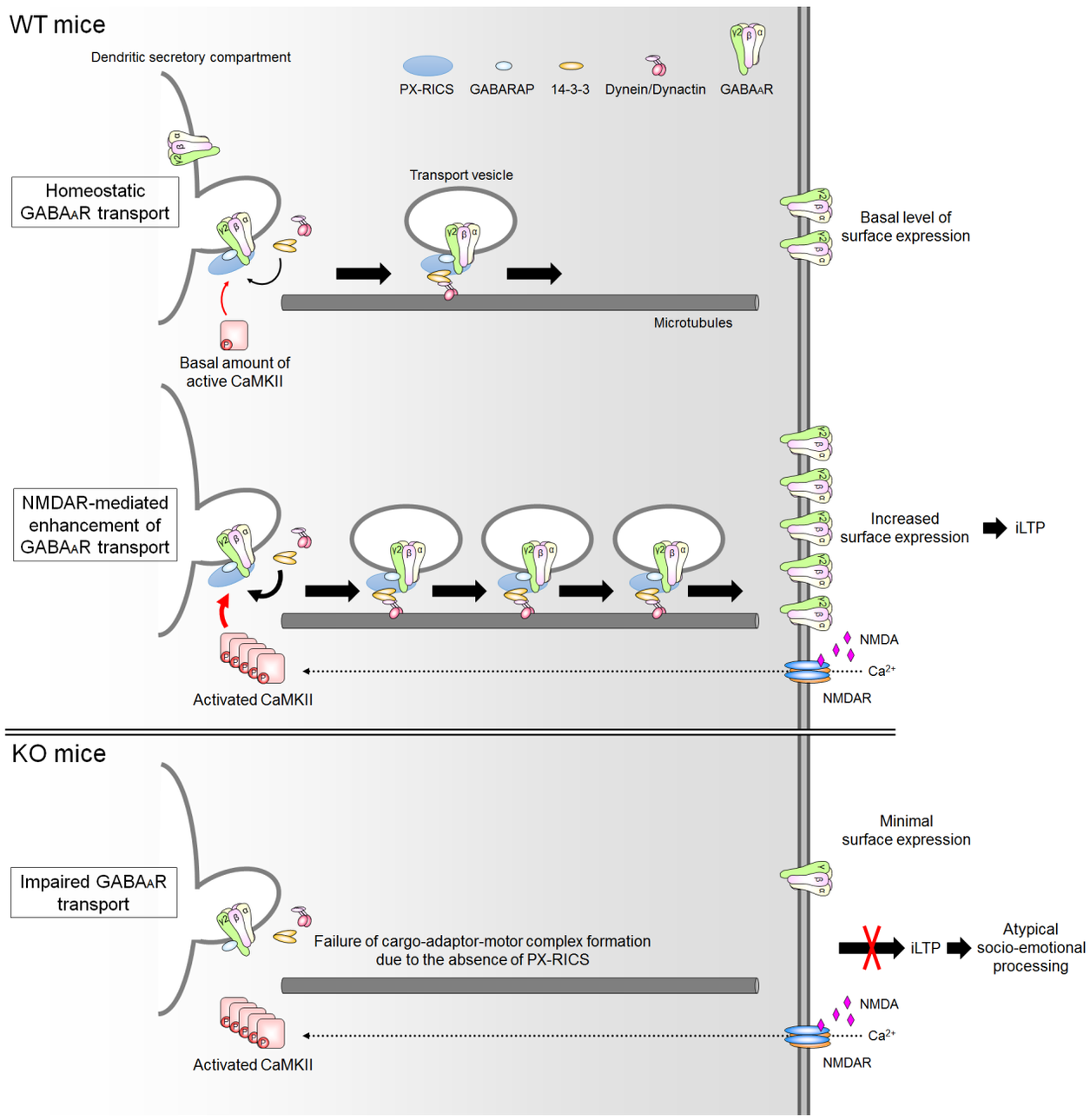
WT mice
Dendritic secretory compartment
PX-RICS
GABARAP
14-3-3
Dynein/Dynactin
GABAAR
Homeostatic GABAAR transport
Transport vesicle
Basal level of surface expression
Microtubules
Basal amount of active CaMKII
NMDAR-mediated enhancement of GABAAR transport
Increased surface expression
iLTP
NMDA
Ca2+
NMDAR
Activated CaMKII
KO mice
Minimal surface expression
Impaired GABAAR transport
Failure of cargo-adaptor-motor complex formation due to the absence of PX-RICS
iLTP
Atypical socio-emotional processing
NMDA
Ca2+
NMDAR
Activated CaMKII

Supplementary Fig. 7. PX-RICS–mediated $GABA_AR$ trafficking underlies NMDAR–dependent GABAergic iLTP

PX-RICS, GABARAP and 14-3-3s are assembled to form an adaptor complex that interconnects γ2-containing $GABA_ARs$ (cargo) and dynein/dynactin (motor). Interaction of PX-RICS with 14-3-3s depends on the phosphorylation activity of CaMKII, and this interaction is a critical regulatory point for $GABA_AR$ trafficking. When CaMKII activity is at a basal level, the PX-RICS–mediated trafficking complex has a role in steady-state transport of $GABA_ARs$ to maintain the number of surface $GABA_ARs$ as needed for proper synaptic inhibition.[3] Neural activity that evokes moderate Ca^{2+} influx through NMDAR preferentially increases the activated form of CaMKII and elicits its translocation to inhibitory synapses,[26] where it phosphorylates target proteins such as gephyrin and the $GABA_AR$ β3 subunit.[37,38,49] Phosphorylated gephyrin and the $GABA_AR$ β3 subunit regulate the surface dynamics of $GABA_ARs$ such as lateral diffusion and synaptic confinement.[37,38,49,58] The present study has revealed that PX-RICS is a downstream CaMKII target associated with anterograde transport of $GABA_ARs$. Enhanced PX-RICS phosphorylation increases the PX-RICS–14-3-3 complex and thereby drives *de novo* $GABA_AR$ surface expression, resulting in GABAergic iLTP. Dysfunction of this trafficking mechanism in the amygdala causes impaired GABAergic synaptic plasticity, which may contribute to deficits in socio-emotional behavior as observed in *PX-RICS/RICS*–deficient mice and JBS patients with autism.

Supplementary Table 1. Summary of the statistical analysis for the behavioral data

Test	Number of mice	Session	Measurement	Genotype	Treatment	Mean	SEM	Statistical test	F value	*P* value	*post hoc* test	Comparison	F value	*P* value	Figure
Fear conditioning	WT = 26 KO = 26	Conditioning	Activity	WT		690.96	31.73	One-way ANOVA	1.94	NS					5B
				KO		774.94	49.08								
			Freezing rate	WT		1.75	0.39	One-way ANOVA	0.56	NS					5C
				KO		1.30	0.46								
		Contextual test	Freezing rate	WT		40.28	3.91	One-way ANOVA	1.56	NS					5D
				KO		33.32	3.97								
			Freezing rate	WT	0–30 s	30.06	3.42	One-way ANOVA	4.72	<0.05					5E
				KO		19.86	3.21								
				WT	30–60 s	36.60	3.79	One-way ANOVA	0.35	NS					
				KO		33.20	4.28								
				WT	60–90 s	45.57	4.77	One-way ANOVA	0.59	NS					
				KO		40.45	4.70								
				WT	90–120 s	44.50	4.69	One-way ANOVA	1.55	NS					
				KO		36.93	3.87								
				WT	120–150 s	47.18	4.62	One-way ANOVA	1.80	NS					
				KO		38.13	4.91								
				WT	150–180 s	46.48	5.38	One-way ANOVA	2.48	NS					
				KO		34.94	4.97								
				WT	180–210 s	36.28	4.73	One-way ANOVA	0.03	NS					
				KO		34.93	5.74								
				WT	210–240 s	40.58	5.49	One-way ANOVA	0.59	NS					
				KO		34.55	5.59								
				WT	240–270 s	39.55	5.37	One-way ANOVA	1.20	NS					
				KO		31.35	5.23								
				WT	270–300 s	36.02	5.00	One-way ANOVA	0.89	NS					
				KO		28.85	5.74								
		Cued test	Freezing rate	WT	Pre-CS	3.57	0.80	Two-way ANOVA	20.86	<0.01	Bonferroni's	WT, Pre-CS vs. CS	116.88	<0.01	5F
				KO		1.71	0.56					KO, Pre-CS vs. CS	18.93	<0.01	
				WT	CS	44.54	4.33					Pre-CS, WT vs. KO	0.24	NS	
				KO		18.20	3.01					CS, WT vs. KO	48.30	<0.01	
			Freezing rate	WT	0–30 s	3.19	1.03	One-way ANOVA	0.92	NS					5G
				KO		1.73	1.11								
				WT	30–60 s	2.57	0.98	One-way ANOVA	0.66	NS					
				KO		1.54	0.75								
				WT	60–90 s	4.17	1.50	One-way ANOVA	1.77	NS					
				KO		1.92	0.72								
				WT	90–120 s	2.49	0.85	One-way ANOVA	0.45	NS					
				KO		1.67	0.86								
				WT	120–150 s	62.44	4.80	One-way ANOVA	21.68	<0.01					
				KO		31.92	4.47								
				WT	150–180 s	58.27	5.10	One-way ANOVA	17.30	<0.01					
				KO		28.46	5.03								
				WT	180–210 s	45.65	4.63	One-way ANOVA	16.90	<0.01					
				KO		19.30	4.44								
				WT	210–240 s	39.03	5.55	One-way ANOVA	16.21	<0.01					
				KO		13.08	3.28								
				WT	240–270 s	32.63	5.19	One-way ANOVA	14.30	<0.01					
				KO		9.61	3.18								
				WT	270–300 s	29.22	5.85	One-way ANOVA	12.96	<0.01					
				KO		6.86	2.10								
Pain sensitivity	WT = 8 KO = 8		Shock intensity	WT	Flinch	0.0250	0.0019	One-way ANOVA	3.50	NS					5H
				KO		0.0200	0.0019								
				WT	Vocalization	0.0488	0.0048	One-way ANOVA	0.03	NS					
				KO		0.0475	0.0053								
				WT	Running/Jumping	0.0825	0.0070	One-way ANOVA	0.72	NS					
				KO		0.0900	0.0053								
Fear conditioning (clonazepam -administered mice)	Vehicle WT = 30 KO = 30 CZP WT = 30 KO = 30	Conditioning	Activity	WT	Vehicle	638.49	37.07	Two-way ANOVA	0.11	NS					6A
				KO		691.81	24.51								
				WT	CZP	569.68	28.10								
				KO		642.14	25.76								
			Freezing rate	WT	Vehicle	2.57	0.67	Two-way ANOVA	0.06	NS					6B
				KO		1.90	0.46								
				WT	CZP	4.25	1.57								
				KO		3.18	0.57								
		Contextual test	Freezing rate	WT	Vehicle	30.33	2.84	Two-way ANOVA	0.62	NS					6C
				KO		20.32	2.69								
				WT	CZP	32.27	3.14								
				KO		27.02	3.35								
			Freezing rate	WT	0–30 s, Vehicle	21.72	3.74	Two-way ANOVA	0.95	NS					6D
				KO		8.06	2.07								
				WT	0–30 s, CZP	25.93	3.39								
				KO		18.66	3.65								
				WT	30–60 s, Vehicle	30.17	3.18	Two-way ANOVA	0.99	NS					
				KO		18.00	2.84								
				WT	30–60 s, CZP	35.83	3.98								
				KO		30.78	4.12								
				WT	60–90 s, Vehicle	36.62	3.09	Two-way ANOVA	0.30	NS					
				KO		26.17	3.77								
				WT	60–90 s, CZP	38.78	3.51								
				KO		32.45	4.50								
				WT	90–120 s, Vehicle	38.43	3.79	Two-way ANOVA	0.48	NS					
				KO		29.17	3.89								
				WT	90–120 s, CZP	40.06	3.58								
				KO		36.34	4.65								
				WT	120–150 s, Vehicle	31.33	3.87	Two-way ANOVA	0.05	NS					
				KO		29.55	4.07								
				WT	120–150 s, CZP	38.95	4.12								
				KO		35.33	4.66								
				WT	150–180 s, Vehicle	32.45	3.90	Two-way ANOVA	0.17	NS					
				KO		23.99	3.52								
				WT	150–180 s, CZP	40.61	4.05								
				KO		28.88	4.56								
				WT	180–210 s, Vehicle	28.34	3.45	Two-way ANOVA	0.08	NS					
				KO		20.01	3.89								
				WT	180–210 s, CZP	30.44	4.14								
				KO		24.28	3.84								
				WT	210–240 s, Vehicle	31.84	4.18	Two-way ANOVA	1.89	NS					
				KO		20.22	4.14								
				WT	210–240 s, CZP	23.16	3.67								
				KO		22.67	4.15								
				WT	240–270 s, Vehicle	26.55	4.06	Two-way ANOVA	1.06	NS					
				KO		15.55	3.37								
				WT	240–270 s, CZP	25.78	4.22								
				KO		23.05	4.31								
				WT	270–300 s, Vehicle	25.83	3.79	Two-way ANOVA	1.09	NS					
				KO		12.50	3.07								
				WT	270–300 s, CZP	23.11	4.62								
				KO		17.72	3.55								
		Cued test	Freezing rate	WT	Pre-CS, Vehicle	4.95	0.98	Two-way ANOVA	1.67	NS					6E
					Pre-CS, CZP	4.07	1.25								
				KO	Pre-CS, Vehicle	0.81	0.32								
					Pre-CS, CZP	2.61	1.04								
				WT	CS, Vehicle	45.03	4.05					Vehicle, WT vs.KO	41.67	<0.01	

				WT	CS, CZP	37.36	4.03	Two-way ANOVA	10.29	<0.01	Bonferroni's	CZP, WT vs. KO	3.69	NS	
				KO	CS, Vehicle	13.40	2.37					WT, Vehicle vs. CZP	2.45	NS	
					CS, CZP	27.96	3.28					KO, Vehicle vs. CZP	8.83	<0.01	
			Freezing rate	WT	0–30 s, Vehicle	4.31	0.99	Two-way ANOVA	3.79	NS					6F
				KO		0.40	0.32								
				WT	0–30 s, CZP	1.61	0.84								
				KO		1.33	1.03								
				WT	30–60 s, Vehicle	6.15	1.85	Two-way ANOVA	3.26	NS					
				KO		0.25	0.18								
				WT	30–60 s, CZP	3.44	0.95								
				KO		2.39	1.20								
				WT	60–90 s, Vehicle	6.84	1.74	Two-way ANOVA	1.92	NS					
				KO		0.65	0.47								
				WT	60–90 s, CZP	5.05	1.87								
				KO		2.83	1.33								
				WT	90–120 s, Vehicle	2.52	0.88	Two-way ANOVA	0.12	NS					
				KO		0.65	0.29								
				WT	90–120 s, CZP	5.11	1.56								
				KO		2.50	1.16								
				WT	120–150 s, Vehicle	65.39	3.92	Two-way ANOVA	9.44	<0.01	Bonferroni's	Vehicle, WT vs.KO	28.56	<0.01	
				KO		33.23	4.42					CZP, WT vs. KO	1.00	NS	
				WT	120–150 s, CZP	58.29	3.92					WT, Vehicle vs. CZP	1.39	NS	
				KO		52.28	4.64					KO, Vehicle vs. CZP	10.02	<0.01	
				WT	150–180 s, Vehicle	59.28	4.16	Two-way ANOVA	10.89	<0.01	Bonferroni's	Vehicle, WT vs.KO	35.89	<0.01	
				KO		21.11	3.67					CZP, WT vs. KO	1.75	NS	
				WT	150–180 s, CZP	49.27	4.72					WT, Vehicle vs. CZP	2.47	NS	
				KO		40.84	5.42					KO, Vehicle vs. CZP	9.59	<0.01	
				WT	180–210 s, Vehicle	46.44	5.15	Two-way ANOVA	9.10	<0.01	Bonferroni's	Vehicle, WT vs.KO	34.18	<0.01	
				KO		9.44	2.29					CZP, WT vs. KO	2.50	NS	
				WT	180–210 s, CZP	36.33	5.38					WT, Vehicle vs. CZP	2.55	NS	
				KO		26.33	4.72					KO, Vehicle vs. CZP	7.12	<0.01	
				WT	210–240 s, Vehicle	36.56	5.13	Two-way ANOVA	5.36	<0.05	Bonferroni's	Vehicle, WT vs.KO	24.49	<0.01	
				KO		6.52	2.02					CZP, WT vs. KO	2.81	NS	
				WT	210–240 s, CZP	26.22	4.83					WT, Vehicle vs. CZP	2.90	NS	
				KO		16.05	4.77					KO, Vehicle vs. CZP	2.47	NS	
				WT	240–270 s, Vehicle	34.05	5.30	Two-way ANOVA	4.71	<0.05	Bonferroni's	Vehicle, WT vs.KO	30.86	<0.01	
				KO		4.75	2.19					CZP, WT vs. KO	6.17	<0.05	
				WT	240–270 s, CZP	19.44	4.52					WT, Vehicle vs. CZP	7.67	<0.01	
				KO		6.33	2.03					KO, Vehicle vs. CZP	0.09	NS	
				WT	270–300 s, Vehicle	28.44	4.88	Two-way ANOVA	3.41	NS	Bonferroni's	Vehicle, WT vs.KO	19.20	<0.01	
				KO		5.35	2.62					CZP, WT vs. KO	3.13	NS	
				WT	270–300 s, CZP	15.22	4.45					WT, Vehicle vs. CZP	6.30	<0.05	
				KO		5.89	2.52					KO, Vehicle vs. CZP	0.01	NS	